Velocity of N_2 upon Dissociation of N_2O in $N_2O{\cdot}(H_2O)_m$

Suketu R. Gandhi*

Institute for Molecular Science, Myodaiji, Okazaki 444−8585, Japan

Received: June 29, 1999; In Final Form: September 20, 1999

Upon dissociating N_2O as a monomer and in $N_2O{\cdot}(H_2O)_m$ ($m = 1-3$), resulting N_2 ($J = 74$) time-of-flight is measured. The photolysis of the complexes proceeds as the two-body dissociation. The fragment's angular distribution is anisotropic. The velocity of N_2 originating from the monomer dissociation is well defined, but those originating from the dissociation in the complexes have their maximum velocity increased up to 36%. This is possible when the kinematic constraints for N_2O dissociation in the complex incorporate the mass of $O{\cdot}(H_2O)_m$ as the counter fragment of N_2. Its implication for a reaction taking place in a complex is discussed.

1. Introduction

Chemical reaction initiated in a weakly bonded complex of RX and ABC (e.g., RX·ABC)[1] is a way to study collision dynamics of oriented molecules[2] with restricted impact parameters. Specifically, upon dissociating RX into R + X, X reacts with, say the "A" end of the molecule that leads to XA + BC.[3,4] In general, results from these studies have shown that the products state distributions of XA/BC are significantly colder than the analogous free atom−molecule reaction.[2−5] Various interpretations of products state distribution, such as formation of a long-lived excited intermediate complex [RX·ABC]*,[6,7] multiple collisions of X with R and ABC,[8] a three body dissociation of R + XA + BC,[9] and a "soft" collision between X and ABC[10] have been forwarded to account for the added complication in the reaction due to the presence of the third body (R).

Any determination of the underlying mechanism involving R requires monitoring of R. When RX and ABC are different, it is possible to identify a fragment's origin from either the dissociative, or the reactive channel, hence elucidating its role in the reaction. Specifically, we show for the first time that the kinematic constraints in the half-collision incorporate the mass of both the fragment and its nearby weakly bonded molecule(s) and that the third body does not participate in the subsequent "collision". This is discerned by a velocity measurement of the nonreactive fragment, here for N_2 upon dissociating N_2O in $N_2O{\cdot}(H_2O)_m$.

In the above explanations,[6−9] an implicit assumption is that upon dissociation of RX in RX·ABC, the translational energy of X is similar to that resulting from the monomer dissociation. The available translational energy (E_{tr}) depends on the incident photon ($h\nu$), the dissociation energies (D_0), and the internal energies (ϵ_{int}) of RX and R + X (E_{int}) through the relation $E_{tr} = h\nu - D_0 + \epsilon_{int} - E_{int}$. For any two-body dissociation, the conservation of energy and momentum gives the following equation for a fragment's translational energy:

$$E_{tr,R} = \frac{m_X}{m_{RX}} E_{tr} \qquad (1)$$

Here $E_{tr,i}$ and m_i are the translational energy and the mass of the particle i, respectively. The maximum $E_{tr,R}$ of the fragment originating from the *complex* is

$$E_{tr,R-max} = \frac{m_{XABC}}{m_{RXABC}} E_{tr} \qquad (2)$$

The validity of (2) would be reflected in the relative increase in the velocity of R. A translational energy of less than the maximum possible would indicate a certain amount of internal energy in the counter fragment (X·ABC). We study N_2O/H_2O because upon dissociation, N_2's velocity in a particular J rotational state resulting from the monomer dissociation is unique, and the mass ratio of N_2's counter fragments [i.e., monomer/complex via eqs 1/2] is sufficiently large to discern any changes in their maximum velocity (22.9%) that may take place. The structure of $N_2O{\cdot}H_2O$ has been determined by both microwave spectroscopy and ab initio calculations, but there is no clear agreement. The experimental structure is that heavy atoms of the molecule form a "T" shape.[11] In contrast, the ab initio study indicates that the complex is planar with one of the H atoms pointing toward the O end of N_2O.[10]

2. Experimental Section

Following is a brief description of the experimental apparatus. A cold beam of N_2O/H_2O is formed by bubbling ca. 2 bar of 4% N_2O in He through H_2O at 16 °C. The mixture is expanded through a pulsed valve (of 475 μs duration). The beam gets transmitted through a 1 mm diameter skimmer, and enters a differentially pumped detector chamber having vacuum of $\sim 5 \times 10^{-7}$ Torr (with the load). Two precision trigger delay generators control the timing of the firing of both the pulsed valve and the laser.

A Nd:YAG/dye laser system generates ~609 nm, which is converted to ~203 nm by use of suitable KDP(I) and BBO(I) crystals. The laser beam is polarized (99% ||-pol with respect to the detection axis) and gets focused by a 350 mm focal length lens. At 10 Hz repetition rate, the laser gives 1.5−1.9 mJ/pulse. A single laser pulse both dissociates N_2O and detects the resulting N_2 in a time-of-flight mass spectrometer (TOFMS).[12−15] The photolysis occurs in an early portion of the laser pulse, while the fragment's detection occurs in an intense portion of the same laser pulse by means of two-photon resonance-enhanced multiphoton ionization of the $a'' \, ^1\Sigma_g^+ \leftarrow X \, ^1\Sigma_g^+$ transition.[16] N_2 detection occurs at the most intense rotational level of $J = 74$, in the Q-branch.[16]

The fragments' velocity can be readily ascertained through their detection in a TOFMS.[13−15] Upon dissociation of randomly oriented N_2O into N_2 ($X \, ^1\Sigma_g^+$) + $O(^1D)$[3] by a polarized laser

* Corresponding author. Mailing address: 342 S. Maple St., Mt. Prospect, IL 60056.

10.1021/jp992232u CCC: $18.00
Published on Web 11/25/1999

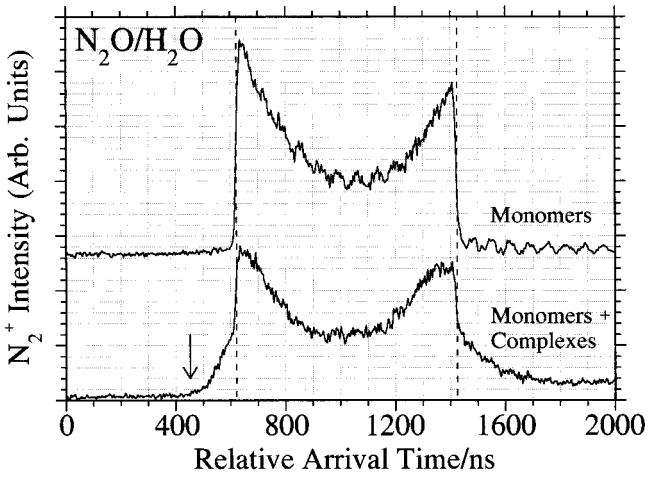

Figure 1. N_2 TOF from the dissociation of N_2O from an early (upper) and a late (lower) portion of the pulsed molecular beam under high resolution condition. The beam consists of monomers in the early portion, and admixtures of monomers and clusters in the late portion. The dashed lines indicate the times of the maximum velocity of N_2 resulting from the monomer dissociation. The arrow above the lower trace indicates onset in the rise of the intensity.

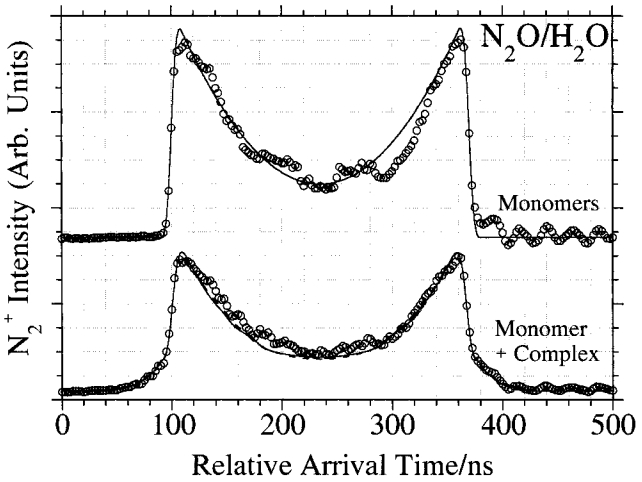

Figure 2. N_2 TOF from the dissociation of N_2O from an early (upper) and a late (lower) portion of the pulsed molecular beam recorded under a lower translational energy resolution than in Figure 1. Raw data (○), computer simulation (—) using parameters in Table 1. (lower trace) Dissociation of an admixture of monomers and clusters. Raw data (○), computer simulations (—) for $\beta_{\text{eff}} = 1.05$, $\beta_{2,\text{eff}} = 0.09_7$, and (- - -) for $\beta_{\text{eff}} = 1.05$, and $\beta_{2,\text{eff}} = 0$. (The differences between the simulations with different $\beta_{2,\text{eff}}$ is negligible.) The velocity and the relative intensities are in Table 2.

along the *z*-axis (i.e., the detection axis), the fragments are ejected toward the $\pm z$ directions with velocity v. Upon their ionization, those ejected upward accelerate (due to the DC *E*-field pointing toward the detector) and arrive at the detector first; those ejected downward first decelerate, and then accelerate toward the detector.[12−15] This causes a spread in the arrival time between fragments of $\pm v$. *E*-fields that were applied to the TOFMS made it possible to record the TOFs in either a higher or a lower translational energy resolution mode. The high (low) translational energy resolution means when the E-fields 31.1 V/2.450 cm (93.2 V/2.450 cm) and 69.2 V/1.075 cm (207.5 V/1.075 cm) were applied to the ionization and the acceleration regions, respectively. The length of the field-free drift region is 28.01 cm. These E-fields satisfy the condition for the space focusing[12,13] so the fragment's arrival time on the detector plane becomes independent of the laser spot size (assuming that the ionization occurs in the center of the ionizer). The detector consists of two microchannel plates (of effective diameter ca. ø30 mm) to amplify the ion signal. This signal is further amplified by two ×10 amplifiers (180 MHz bandwidth) then recorded by a digital oscilloscope (350 MHz bandwidth) every 2.5 ns and averaged for 1000 (250) pulses for the higher (lower) translational energy resolution.

3. Results and Discussions

Figure 1 shows N_2^+ time-of-flight (TOF) from the dissociation of N_2O from both an early (upper) and a late portion (lower) of the pulsed molecular beam recorded under the high translational energy resolution. The uneven intensities between the "upward" and the "downward" ejected fragments arise because the XY deflection voltages were not optimized. In other words, there is a nonsymmetric ion collection efficiency about the *z*-axis. The upper trace results from the dissociation of N_2O in an early portion of the beam. The sharp rise and fall in the intensity is consistent with a sharp velocity distribution, as is expected from the monomer dissociation. The lower trace of the TOF originates from the dissociation from a late portion of the pulse. The conspicuous difference between them is the increase in the width for the TOF.

Additional pressure dependence (which ranged from ∼0.4−3 bar) TOF of N_2^+ were taken (but they are not shown) to ascertain the origin of the increase in the width. Upon increasing the stagnation pressure, the TOF spectra from the dissociation in the early portion remained unchanged. In contrast, the TOF spectra originating from the dissociation in the late portion of the beam changed as the stagnation pressure changed. As the pressure increased, the shoulders became wider and its relative intensity with respect to the monomer peaks increased. This is attributed to the presence of N_2O as complexes in the late portion of the beam, while the early portion consists of monomers.

The principal difference between the TOFs upon dissociating N_2O in the early and the late portion of the pulse is the increase in the N_2^+ width. The width of the TOF originating from the monomer dissociation is ∼800 ns; the onset in the increase of the intensity for the TOF originating from the dissociation of the clusters occurs ∼170 ns earlier, which corresponds to ∼40% increase in the velocity of N_2. Because of the "unsymmetric" ion collection efficiency about the *z*-axis, a computer simulation is not possible. Therefore, it was necessary to decrease the resolution, hence the *E*-fields in the TOF were increased (by ×3). Figure 2 shows the data recorded under this condition.

The upper trace of Figure 2 shows that the TOF of N_2^+ originating from the monomer dissociation is anisotropic as expected.[16,17] The N_2^+ TOF is essentially the *z*-component of the velocity (v_z) of its precursor N_2, which indirectly reflects the fragment's angular distribution.[14,15] A computer simulation of N_2^+ TOF (Figure 2) enables one to extract both the "effective" anisotropy parameters and the magnitude of the velocities (v) which describe its angular distribution,[18,19]

$$I(v_z/v) = 1 + \beta_{\text{eff}} P_2(v_z/v) + \frac{72}{35}\beta_{2,\text{eff}} P_4(v_z/v) \qquad (3)$$

$I(v_z/v)$ is the observed intensity, β_{eff} and $\beta_{2,\text{eff}}$ are the effective anisotropy parameters for photofragments originating from randomly oriented molecules (as for the notation of ref 19b), and $P_2(v_z/v)$ and $P_4(v_z/v)$ are second and fourth order Legendre's polynomial.

A simulation of a fragment's TOF using the well-known equations[12,13] (with the above experimental parameters) and convoluting the ion's arrival time with a realistic laser pulse

TABLE 1: Parameters Extracted from the TOF of N_2 ($J = 74$) from Monomer Dissociation (Figure 2, Upper Panel)

$v = 1.76_5$ km/s
$\beta_{eff} = 1.05 \pm 0.10$
$\beta_{2,eff} = 0.09_7 \pm 0.04_9$

duration (i.e., a Gaussian instrument response function, fwhm = 8.5 ns) gives v, β_{eff}, and $\beta_{2,eff}$ (cf. Table 1). $\beta_{eff} = 1.05$ is close to the previously reported value (1.0) based on $O(^1D)$ detection.[17c] N_2's velocity extracted from the simulation is 1.76_5 (± 0.015) km/s; the uncertainty reflects the range that can be fitted to the data upon inspection. The calculated v for N_2, using the photon energy (6.105 eV) and D_0 (3.641 eV)[20] is 1.67_3 km/s. The discrepancy between the calculated and the measured v arises due to neglect of the higher order spectroscopic constants in computing E_{int} for high J states of N_2. Since the calculated E_{tr,N_2} is lower than its observed value, it implies that the rotational energy of N_2 ($J = 74$) is also lower than its calculated value using the known spectroscopic constants[21a] and by setting $\epsilon_{int} = 0$. That is, in a cold supersonic expansion, we expect more than 90% of N_2O's population resides in $J \leq 13$ or $E_{rot} < 65$ cm^{-1} (assuming that the rotational temperature = 50 K). Therefore, setting $\epsilon_{int} = 0$ for the computational purpose, E_{tr} causes a negligible error. (We note that both the rise and the fall times of the intensity are very sharp, which result in high-frequency ringing. This ringing is an artifact.)

The TOF originating from the dissociation of the complexes (lower traces of Figures 1 and 2) consistently have wider distributions than those originating from the monomer dissociation (upper traces of Figures 1 and 2) regardless of the *E*-fields of the TOFMS. Upon increasing the *E-fields* of the TOFMS, the XY deflection voltages were optimized, hence the ion collection efficiency improves (i.e., Figure 2). This makes it possible to carryout a computer simulation of the data to extract the fragments velocities. The simulation uses multiple velocities and sets $\beta_{eff} = 1.05$ with $\beta_{2,eff} = 0$ and 0.09_7. (This is justified since the anisotropy in the angular distribution of N_2 originating from the complex would not be greater than that of the monomers.) A simulation was first fitted on the outer edges of the intensity (i.e., the maximum velocity of N_2). When the fit was satisfactory reproduced, an intensity of a smaller velocity (in increments of 25 m/s) was added to ascertain if its contribution to the TOF intensity improves the fit. This step was repeated for a number of velocities. (We note that for $v_{N_2} > 1.8$ km/s in the horizontal direction, the collection efficiency due to finite aperture of the detector is less than 100%.) On obtaining "zeroth" order intensities, they were further varied to improve the fit. Table 2 gives the relevant parameters used in the fit.

Upon varying the intensities within 25% for the velocities of $N_2 > 1765$ m/s, the fit did not change drastically. On the other hand, the fit changed as the intensities were varied more than 25%. The intensities of those N_2 having velocities less than that of the monomers, there were no unique sets of velocities/intensity parameters that reproduced the TOF. Specifically, variations in the intensity of each of the velocities between 1600 and 1750 m/s did not result in discernible change in the fit when the sum of the intensities was constant. This is not surprising, as the smaller velocity components are buried under the intense monomer peak, and therefore not very sensitive to the variation in the intensity. In addition, the difference between the fit of $\beta_{2,eff}$ of the monomer and $\beta_{2,eff} = 0$ are insignificant. While the simulation reasonably reproduces the outer edges of the TOF, the center intensity is lower than the observed. This should not be surprising, as we do not have any size selectivity, and thus it is not possible to know the precise value of the anisotropy parameters.

TABLE 2: Parameters Used in Computer Simulations of the TOF of N_2 ($J = 74$) from the Dissociation of an Admixture of Monomer and the Complex (i.e., Figure 2, Lower Panel)[a]

N_2 velocity (m/s)	relative intensity	m[b]
1625	2.0	1,2,3
1675	4.5	1,2,3
1700	13	1,2,3
1725	14	1,2,3
1765[c]	41	0
1925	6.0	1,2,3
1950	6.0	1,2,3
2100	7.5	1,2,3
2250	2.3	2,3
2400	3.3	3

[a] β_{eff} is same as in the monomer, and $\beta_{2,eff}$ in the simulation are 0 and 0.09_7. [b] Origin from clusters of $N_2O{\cdot}(H_2O)_m$ [c] β_{eff} and $\beta_{2,eff}$ used are the same as in the monomer dissociation.

The key point made here is the increase in the maximum N_2 velocity originating from complexes relative to that from the monomers by 36%, which is comparable to the increase of ~40% for the maximum velocity from the data in Figure 1. This observation cannot be explained by the mechanisms forwarded to account for colder product state distributions.[6-9] Formation of N_2 ($J = 74$) from a long-lived excited complex is excluded. If $[N_2O{\cdot}H_2O]^*$ had a "long lifetime", it could be ionized by the absorption of two photons. (The ionization potentials of N_2O/H_2O are 12.85 eV/12.62 eV.[21b] We estimate the ionization energy of $N_2O{\cdot}H_2O = 12.85$ eV.) No detection of ions in the range 45 $(N_2OH)^+ \leq m/z \leq 62$ $(N_2O{\cdot}H_2O)^+$ occurred that would give an evidence of the excited complex. We note that in a separate experiment both N_2O^+ and H_2O^+ were detected; their temporal widths were ~10 ns, which is comparable to ~7 ns fwhm (of scattered laser pulses on the detector). Furthermore, there was no shoulder near their baseline. If the detected N_2O^+/H_2O^+ had resulted from the complex's fragmentation, their width (including that near the baseline) should have been significantly broader than ~10 ns to account for their velocity.

To determine the contribution of N_2 TOF originating from the complexes, we subtract a fraction of the monomers TOF from that of the admixture of monomers and clusters. The fraction of the monomer's intensity that needs to be subtracted remains unknown, but both an "upper" and a "lower" limit of the TOF spectrum originating from the complex can determined. The fractions used to subtract the monomer intensity from that of the admixture were 0.45 and 0.65; the TOF range originating from the complex are shown in Figure 3. These fractions give the TOF intensity > 0 and a "smooth" spectrum near the onset in the increase in the intensity near the maximum velocity of N_2 from the monomer dissociation (i.e., ~100 ns and ~370 ns in Figure 3).

We note that the angular distribution of N_2 ($J = 74$) originating from the complex appears to be anisotropic. The reason being that <100% collection efficiency for those molecules having $v \geq 1800$ m/s which gives appearance of anisotropic. To ascertain whether the angular distribution is truly anisotropic, another computer simulation (which is not shown) was made. In this simulation we assumed that $\beta_{eff} = 0$. Both the velocity and the intensity parameters used were the ones that fitted the "outer edges"; they were those in Table 2 and "redetermined" (with exception of that of the monomer). (The procedures used to determine velocity and intensity parameters,

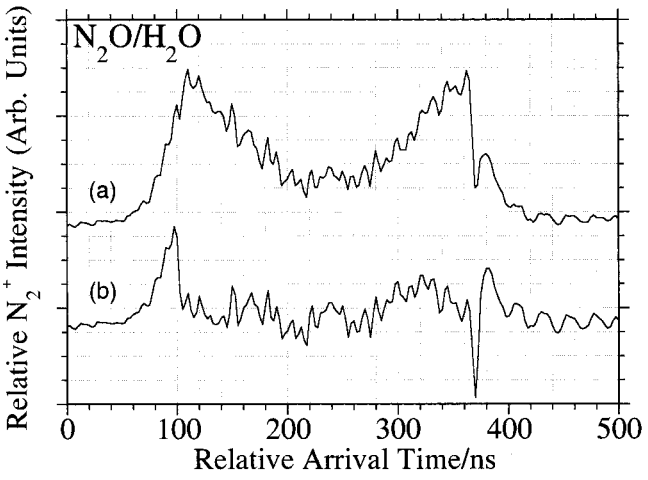

Figure 3. Range of N_2 TOF from the dissociation of clusters obtained upon subtracting 0.45 (a) and 0.65 (b) multiplied by the monomer TOF from that of the admixture of Figure 2.

for $\beta_{eff} = 0$, were the same as discussed previously.) These simulations satisfactorily reproduced the "outer edges" of the TOF spectrum, but not the inner portion. Specifically, the simulation showed that the intensity in the inner part (i.e., TOF in the range ~200−300 ns) was either too flat (using the parameters in Table 2) or significantly more intense than the observed TOF. For these reasons, it is concluded that the TOF of N_2 originating from the dissociation of the complex is truly anisotropic.

Simultaneous three-body dissociation of $[N_2O{\cdot}H_2O]^*$ resulting into either N_2 ($J = 74$) + O + H_2O (i.e., nonreactive channel) or N_2 ($J = 74$) + OH + OH (reactive channel) is unlikely. The evidences suggesting that a two-body dissociation taking place is based on the observation of rotationally excited N_2 (i.e., $J = 74$), and the anisotropy in the angular distribution. If a three-body dissociation was taking place, we certainly expect different torque to have been exerted on N_2, and the fragment would have remained undetected in this high rotational state. Furthermore, the derivation of the anisotropy in the angular distribution results from a two-body dissociation process.[18] It is not at all clear whether such anisotropy should exist in a three-body dissociation.

An additional reason to discount the three-body dissociation process is attributed to the velocity of the N_2. If the qualitative trends (as discussed theoretically) for a three-body dissociation[22] are applicable here, we expect N_2 ($J = 74$) to have a wide range of velocities. The increase in N_2 velocity is readily discerned (i.e., $v > 1765$ m/s), but its low velocity in the range of 0−0.25 eV (or 0−1250 m/s) is not evident. That is, for the low velocities, apparent intensity is $\propto 1/v$, but there is no evidence of intense peaks in the center region of Figure 3. In view of this, and the fact that the angular distribution of N_2 is anisotropic and detecting rotationally excited N_2 ($J = 74$), we do not have any evidence to believe that three-body dissociation takes place.

A multiple collision of O with H_2O/N_2 does not arise.[8] The kinematics of a two-body collision of O with stationary $(H_2O)_m$ results in the reversal of its velocity in the laboratory frame to ~0.2, 1.2, and 1.6_8 km/s for $m = 1$, 2, and 3, respectively. These velocities are too slow for O to catch up with the faster N_2 ($v = 1.76_5$ km/s).

A possibility of increase in N_2 ($J = 74$) velocity from $N_2/O(^3P)$ does not arise. If a portion of N_2 ($J = 74$) had resulted from this channel, onset in the intensity (in the absence of the kinematic constraint) would have occurred ~2700 m/s or ~3300 m/s (with the kinematic constraint for $N_2O{\cdot}H_2O$). We do not see any increase in the intensity in the TOF data obtained either in high resolution (i.e., Figure 1) or the low resolution (Figure 2). Even with certain amount of internal excitation of the intermediate complex, there should have been certain intensity of N_2 ($J = 74$) at the time corresponding to the "threshold velocity". Failure to detect this implies that N_2 ($J = 74$) reaches its asymptotic limit with $O(^1D)$.

In this experiment, N_2O and H_2O were co-expanded, but there is no direct information on the cluster composition of N_2O as $(N_2O)_n$ or $(N_2O)_n{\cdot}(H_2O)_m$. We can rule out the possibility of discernible abundance of $(N_2O)_n$ ($n \geq 2$) since it is known that, upon dissociation, its fragments are NO[3]. NO can be readily detected as NO^+ at 203 nm.[21a] Our failure to detect NO^+ implies that N_2 originates from either N_2O or $N_2O{\cdot}(H_2O)_m$.

The increase in the velocity of N_2 is adequately accounted when the kinematic constraints incorporate mass of its counter fragment which includes that of nearby H_2O via eqs 2. The origin of various cluster sizes of N_2 remains undetermined, as we do not have any size specificity. On the basis of the (i) kinematic constraints [i.e., eq 2], (ii) limit that the D_0 of N_2-O with $(H_2O)_m$ is the same as that of the monomer, and (iii) that a negligible amount of binding energy of N_2O and $(H_2O)_m$ couples into fragment's translational energy, we identify all of the possible origins of the N_2 on the cluster in Table 2. The ambiguity cannot be eliminated in this experiment, as there is no size selectivity of the complexes. On the other hand, we can estimate the extreme limits (i.e., the minimum and the maximum amount) of the internal energy in the fragments on the basis of assignments in Table 2: 70−700 meV for $O{\cdot}(H_2O)_3$; 110−650 meV for $O{\cdot}(H_2O)_2$; 75−540 meV for $O{\cdot}H_2O$.

Existence of the kinematic constraints incorporating the masses of O and $(H_2O)_m$ means that the relative velocity of the reactive reagents with respect to each other is certainly smaller than the moving atom/stationary molecule, but remains undetermined. This supports the conjecture that the collision of $O(^1D)$ with H_2O is "soft",[10] but the excess energy of the intermediate is *not* dissipated in N_2. Our direct observation of the increase in a nonreactive fragment's velocity has been noted in a theoretical study by Kulda and Schatz[23] on the reaction H + $CO_2 \rightarrow$ OH + CO upon dissociation of HBr in $HBr{\cdot}CO_2$. They found that the average E_{tr} of Br originating from the complex increases by 10% relative to that of HBr dissociation, but smaller than the maximum of 36%.

The above conclusion gives rise to a different picture of the oriented molecule collision. When a molecule dissociates, a fragment's translational energy depends on the mass of its counter fragment *and* the nearby atoms/molecules. The translational energy of X as "seen" by ABC is *not* that which results from dissociation of an isolated RX, i.e., X moving, while ABC remains stationary. The reason is that, during the dissociation process, both X and ABC move *together*, as depicted in Figure 4. In our case, the atom $(O,^1D)$ collides with oriented molecule (H_2O) upon dissociation of N_2O. The origin of the detected N_2 from the complexes is consistent with the fact that its complementary fragment has a mass heavier than that of O. This should not be surprising since the interactions between O and H_2O are attractive, as they are highly reactive.[24] This is the first sequence as a two-body dissociation prior to the eventual reaction. The translational energy of the atom reacting with the nearby molecule remains unknown, but it is not at all clear whether the amount of the internal energy in $O{\cdot}H_2O$ is an equivalent to the collisional energy. For this reason, comparisons of reactions between the free gas-phase and analogous weakly bonded

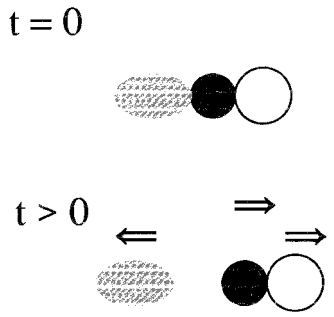

Figure 4. Cartoon of a two body dissociation taking place in a weakly bonded complex. Both the fragment and the nearby molecule move as the bond breaks.

complex are inappropriate unless the translational energy of reagents in the center of the mass reference frame is low.

Closely related to this work is the reaction initiated in $O_3 \cdot CH_4$[25a] and $N_2O \cdot CH_4$[25b] upon dissociation of O_3 and N_2O at 266 nm and 193 nm, respectively, that produces OH and CH_3. They observed high rotational states of OH, which is similar to the corresponding reaction between free O and CH_4. For this reason, it has been concluded that the dissociation process occurs as the first step in the two-body process. We point out that it is the nonreactive fragment that gives information on the role that it may play in the subsequent reaction. Furthermore, an additional difference between the free gas-phase collision and reaction initiated in the weakly bonded complex is on the nature of collisional energy, which remains undefined. That is, both the fragment of interest and nearby surrounding molecule move during the dissociation process (cf. Figure 4). Thus, velocity remains undetermined.

Our conclusions are for the dissociation (or half-collision) process, but they are consistent with full-collision experiments involving atoms/molecules held together by weak forces. Interpretations of the reactive collisions of $K + (Cl_2)_2$ by Herschbach[26a] and $Rb + (CH_3I)_6$ by Bernstein[26b] were possible when the kinematic constraint incorporated the mass of entire clusters. A more elegant experiment by Buck and Meyer[27] is scattering of He from Ar_n ($n = 1-3$), where Ar_n does *not* dissociate. In that experiment, a beam of Ar_n was scattered with a certain center of mass velocity. One attains the size selection upon the detection of a velocity-selected Ar_n at a specific laboratory angle. In order for this size selection of clusters to occur by the collisional means, the existence of the kinematic constraints must hold for atoms bounded by the weak van der Waals forces, as it is for atoms held together by strong chemical forces.

Furthermore, enhancement of fragment velocities upon photodissociation of molecules physiadsorbed on surfaces has been observed previously, but the underlying explanations have differed. In the photodissociation of CH_3Br at 193 nm experiment by Cowin,[28a] they had observed that the Br velocity was significantly higher than possible from free gas-phase dissociation. This increase in velocity was attributed to "multiple" collisions of recoiling CH_3 that eventually collides with slow moving Br. Similar observations were made by Welge upon dissociation of CH_3I at 266 nm and detection of I* ($^2P_{1/2}$) atom.[28b] As with Cowin, the velocity of I* was beyond that expected from free gas-phase dissociation. They attributed this to the kinematics, i.e., counter fragment of I* is significantly heavier than CH_3. While the comparison between our observation on the enhancement on the fragment velocity originating from the complex with the work of Cowin[28a] and Welge[28b] can be made, the underlying reason for this is consistent with that given by the latter.

Furthermore, we can extend the above conclusion to the picture of dissociation of a molecule taking place in a solvent cage in either a cluster or a liquid[5c,29] which leads to reinterpretation of the process. Specifically, *during* the dissociation process, both the fragments and nearby solvent(s) *move* (cf. Figure 4). This means that the dissociation process would be slower in comparison when comparing that of an isolated molecule. This slowing down is not attributed to the collisions with the stationary "cage", but due to the "effective" mass being heavier. The effective mass is the mass of a fragment and its surrounding weakly bonded molecules. In other words, given a comparable amount of E_{tr} in both the gas and solution phases, as the effective mass increases, the velocity of the fragments and nearby solvent automatically decrease. This view contrasts with the accepted[30] notion on the cage effect that the dissociation of molecules is fast, as in the gas phase, but the fragments get slowed due to collisions with the nearby solvent.

Acknowledgment. S.R.G. is grateful to both Dr. Y. Mo and Prof. G. Schatz and to one of the referees for useful comments and discussions, and to Japan Society for the Promotion of Science for an award of the Research Fellowship (1994-95) when this work was initiated.

References and Notes

(1) Jouvet, C.; Soep, B. *Chem. Phys. Lett.* **1983**, *96*, 426.
(2) (a) Parker, D. H.; Bernstein, R. B. *Annu. Rev. Phys. Chem.* **1989**, *40*, 561. (b) Loesch, H. J. *Annu. Rev. Phys. Chem.* **1995**, *46*, 555.
(3) (a) Honma, K.; Kajimoto, O. *Chem. Phys. Lett.* **1985**, *117*, 123. (b) Honma, K.; Fujimura, Y.; Kajimoto, O.; Inoue, G. *J. Chem. Phys.* **1988**, *88*, 4739.
(4) (a) Buelow, S.; Radhakrishnan, G.; Catanzarite, J.; Wittig, C. *J. Chem. Phys.* **1985**, *83*, 444. (b) Radhakrishnan, G.; Buelow, S.; Wittig, C. *J. Chem. Phys.* **1986**, *84*, 727.
(5) (a) Takayanagi, M.; Hanazaki, I. *Chem. Rev.* **1991**, *91*, 1193. (b) Shin, S. K.; Chen, Y.; Nickolaisen, S.; Sharpe, S. W.; Beaudet, R. A.; Wittig, C. *Adv. Photochem.* **1991**, *16*, 249. (c) Gerber, R. B.; McCoy, A. B.; Garcia-Vela, A., *Annu. Rev. Phys. Chem.* **1994**, *45*, 275.
(6) Scherer, N. F.; Sipes, C.; Bernstein, R. B.; Zewail, A. H. *J. Chem. Phys.* **1990**, *92*, 5239.
(7) Shin, S. K.; Wittig, C.; Goddard, W. A., III *J. Phys. Chem.* **1991**, *95*, 8048.
(8) Wittig, C.; Engel, Y. M.; Levine, R. D. *Chem. Phys. Lett.* **1988**, *153*, 411.
(9) King, D. S.; Sauder, D. G.; Casassa, M. P. *J. Chem. Phys.* **1994**, *100*, 4200.
(10) Tanaka, N.; Nagashima, U.; Takayanagi, M.; Kim, H. L.; Hanazaki, I. *J. Phys. Chem.* **1997**, *101*, 507.
(11) Zolandz, D.; Yaron, Y.; Peterson, K. I.; Klemperer, W.; I. *J. Chem. Phys.* **1992**, *97*, 2861.
(12) Wiley, W. C.; McLaren, I. H. *Rev. Sci. Instrum.* **1955**, *26*, 1150.
(13) Franklin, J. L.; Hierl, P. M.; Whan, D. A. *J. Chem. Phys.* **1967**, *47*, 3148.
(14) Mons, M.; Dimicoli, I. *Chem. Phys. Lett.* **1986**, *131*, 298.
(15) Gandhi, S. R.; Curtiss, T. J.; Bernstein, R. B. *Phys. Rev. Lett.* **1987**, *59*, 2951.
(16) Hanisco, T. F.; Kummel, A. C. *J. Phys. Chem.* **1993**, *97*, 7242.
(17) (a) Felder, P.; Haas, B.-M.; Huber, J. R.; *Chem. Phys. Lett.* **1991**, *186*, 177. (b) Springsteen, L. L.; Satyapal, S.; Matsumi, Y.; Dobeck, L. M.; Houston, P. L. *J. Phys. Chem.* **1993**, *97*, 7239. (c) Suzuki, T.; Katayanagi, H.; Mo, Y.; Tonokura, K. *Chem. Phys. Lett.* **1996**, *256*, 90.
(18) Yang, S.; Bersohn, R. *J. Chem. Phys.* **1974**, *61*, 4400.
(19) (a) Dixon, R. N.; *J. Chem. Phys.* **1986**, *85*, 1866. (b) Mons, M.; Dimicoli, I. *J. Chem. Phys.* **1989**, *90*, 4037.
(20) Chase, M. W.; Davies, C. A.; Downey, J. R.; Frurip, D. J.; McDonald, R. A.; Syverud, A. N. JANAF Thermochemical Tables, 3rd ed. *J. Phys. Chem. Ref. Data* **1985**, *14* (Suppl. 1).
(21) (a) Huber, K. P.; Herzberg, G. *Constants of Diatomic Molecules*; Van Nostrand: New York, 1979. (b) Herzberg, G. *Electronic Spectra and Electronic Structure of Polyatomic Molecules*; Van Nostrand: New York, 1967.
(22) Strauss, C. E. M.; Houston, P. L. *J. Phys. Chem.* **1990**, *94*, 8751.
(23) Kudla, K.; Schatz, G. C. *J. Phys. Chem.* **1991**, *95*, 8267.
(24) Butler, J. E.; Talley, L. D.; Smith, G. K.; Lin, M. C. *J. Chem. Phys.* **1981**, *74*, 4501.

(25) (a) Van Zee, R. D.; Stephenson, J. C.; Casassa, M. P. *Chem. Phys. Lett.* **1994**, *223*, 167. (b) Wada, S.; Obi, K., *J. Phys. Chem. A* **1998**, *102*, 3481.

(26) (a) King, D. L.; Dixon, D. A.; Herschbach, D. R. *J. Am. Chem. Soc.* **1974**, *96*, 3328. (b) Gonzáles Ureña, A.; Bernstein, R. B.; Phillips, G. R. *J. Chem. Phys.* **1975**, *62*, 1818.

(27) (a) Buck, U.; Meyer, H. *Phys. Rev. Lett.* **1984**, *52*, 109. (b) Buck, U. *J. Phys. Chem.* **1988**, *92*, 1023.

(28) (a) Tabares, F. L.; Marsh, E. P.; Bach, G. A.; Cowin, J. P. *J. Chem. Phys.* **1987**, *86*, 738. (b) Kutzner, J.; Lindeke, G.; Welge, K. H. *J. Chem. Phys.* **1989**, *90*, 548.

(29) Franck, J.; Rabinowitsch, E., *Trans. Faraday Soc.* **1934**, *30*, 120.

(30) (a) Harris, A. L.; Brown, J. K.; Harris, C. B. *Annu. Rev. Phys. Chem.* **1988**, *39*, 341. (b) Nadal, M. E.; Kleiber, P. D.; Lineberger, W. C. *J. Chem. Phys.* **1996**, *105*, 504.